STRUCTURAL STUDIES OF SOME NATURAL PRODUCTS FROM KAEMPFERIA PARVIFLORA, IRIS GERMANICA LINN. AND ANDROGRAPHIS PANICULATA NEES

JEANNIE TEH BEE JAN

UNIVERSITI SAINS MALAYSIA
2007

STRUCTURAL STUDIES OF SOME NATURAL PRODUCTS FROM KAEMPFERIA PARVIFLORA, IRIS GERMANICA LINN. AND ANDROGRAPHIS PANICULATA NEES

by

JEANNIE TEH BEE JAN

Thesis submitted in fulfilment of the requirements
for the degree of
Master of Science

June 2007

ACKNOWLEDGEMENTS

God, thank you for this day and the blessings you have given me. It is your strength that pushed me forward to become a better person in life. To my family members, thank you so much for believing in me and giving me the freedom, encouragement and support in pursuing my dreams. Thanks for being there through my thick and thin.

Special thanks is due to my supervisor, Prof. Fun Hoong Kun and my co-supervisor, Dr. Abdul Razak Ibrahim for their professionalism, indispensable guidance, patience and unconditional commitment throughout this research. It was a new learning experience and I was indeed lucky to be a member of X-ray crystallography lab.

Appreciation is extended to fellow researchers from Malaysia, Thailand and Pakistan for their help, especially in producing research samples and full cooperation in writing up papers for publications in Acta Cryst E. In addition, I would like to express my heartfelt gratitude to the Malaysian Government and Universiti Sains Malaysia (USM) for the post of research officer through the Scientific Advancement Grant Allocation (SAGA) grant No. 304 / PFIZIK / 653003 / A118 and Science Fund grant No. 305 / PFIZIK / 613312 which have contributed largely to the success of this research.

Special acknowledgement is due to Institute of Graduate Studies (IPS) for giving me the chance to further my studies up to this level. I am also thankful to be given the opportunity to use the facilities at School of Physics, USM.

Last but not least, I would like to sincerely thank Mr. Karuna and my fellow friends for their warm hospitality and cooperation throughout my studies in X-ray crystallography lab. It is my pleasure to work with all of them and I shall always cherish the moments we have shared together.

TABLE OF CONTENTS

CHAPTER 2 - BASICS OF X-RAY STRUCTURE ANALYSIS

CHAPTER 3 - MATERIALS AND METHODS

LIST OF TABLES

LIST OF FIGURES

LIST OF PLATES

LIST OF ABBREVIATIONS

CCD	Charge-Coupled Device
R	Reliability Index
SADABS	Siemens Area Detector Absorption Correction
SAINT	SAX Area-detector Integration (SAX-Siemens Analytical X-ray)
SMART	Siemens Molecular Analysis Research Tools
wR	Weighted Reliability Index

KAJIAN STRUKTUR BEBERAPA PRODUK SEMULAJADI DARIPADA TUMBUH-TUMBUHAN KAEMPFERIA PARVIFLORA, IRIS GERMANICA LINN. DAN ANDROGRAPHIS PANICULATA NEES

ABSTRAK

Dalam kajian ini, struktur hablur untuk lima produk semulajadi telah ditentukan melalui kaedah kristalografi sinar-x hablur tunggal. Data hablur diperolehi dengan menggunakan alat difraktometer *APEX-2 CCD* (Bruker, 2005). Data suhu rendah diambil dengan menggunakan sambungan suhu rendah Oxford Cryosystem Cobra. Struktur-struktur kemudiannya ditentukan dan dihaluskan dengan bantuan perisian *SHELXTL* (Sheldrick, 1998). Perisian ini juga membenarkan kita melihat susunan molekul-molekul di dalam hablur dan mengenalpasti susunan ikatan-ikatan yang terlibat di dalamnya. Huraian tentang struktur-struktur yang telah diselesaikan adalah seperti berikut :-

Hablur 3,5,7 – Trimethoxy – 2 – phenyl - 4*H* – 1 – benzopyran – 4 – one mempunyai kumpulan ruang $P2_1/c$. Struktur hablur distabilkan oleh interaksi π-π di antara sistem gelang benzopyran – 4 - one bagi molekul-molekul yang berhubung secara songsang serta disusun sepanjang paksi *a*. Interaksi C-H…O meningkatkan lagi kestabilan padatan hablur.

Sebatian 5 – Hydroxy – 7 – methoxy – 2 - (4 - methoxyphenyl) - 4*H* – 1 benzopyran – 4 – one menghablur dalam kumpulan ruang $P2_1/c$. Sistem gelang benzopyran – 4 - one dan rangkaian methoxyphenyl adalah hampir sesatah.

Molekul-molekul adalah dihubungkan melalui ikatan-ikatan hidrogen C-H…O untuk membentuk rantaian sepanjang paksi *a*.

Struktur hablur 5,7 – Dimethoxy - 2-phenyl - 4*H* – 1 – benzopyran – 4 - one chloroform solvate distabilkan oleh interaksi π-π di antara sistem gelang benzopyran – 4 - one bagi molekul-molekul yang berhubung secara songsang serta disusun sepanjang paksi *c*. Interaksi C-H…O dan C-H…π menambahkan lagi kestabilan padatan hablur. Hablur ini mempunyai kumpulan ruang $P2_1/c$.

Sebatian 4’ – Hydroxy – 5 – methoxy - 6,7 – methylenedioxyisoflavone membentuk rantai infiniti zigzag satu dimensi yang berkembang selari kepada paksi *b* melalui ikatan-ikatan hidrogen O-H…O. Rantaian tersebut disusun sepanjang paksi *c*. Interaksi lemah π-π and C-H…π meningkatkan lagi kestabilan struktur hablur. Sebatian ini menghablur dalam kumpulan ruang $P2_1/c$.

Sebatian 14 – Deoxy - 11,12 – didehydro - 3,19 – isopropylideneandrographolide mempunyai kumpulan ruang $P2_12_12_1$. Kesemua gelang segienam di dalam struktur menunjukkan konformasi kerusi. Struktur hablur distabilkan oleh interaksi C-H…O yang membentuk jaringan dua dimensi selari kepada satah *ab*.

STRUCTURAL STUDIES OF SOME NATURAL PRODUCTS FROM KAEMPFERIA PARVIFLORA, IRIS GERMANICA LINN. AND ANDROGRAPHIS PANICULATA NEES

ABSTRACT

In this research, single crystal x-ray crystallography method had been used to determine the crystal structures of five natural products. The data was collected using the *APEX-2 CCD* diffractometer (Bruker, 2005). Low temperature data were collected using the Oxford Cryosystem Cobra low-temperature attachment. The structures were then solved and refined by the use of *SHELXTL* (Sheldrick, 1998) software. This software also allows us to see the arrangement of molecules in the crystal and the packing interactions involved. Details of the solved structures are given below:-

The structure of 3,5,7 – Trimethoxy – 2 – phenyl - 4*H* – 1 – benzopyran - 4 – one crystallizes in the space group of $P2_1/c$. The crystal structure is stabilized by π-π interactions between the benzopyran – 4 - one ring systems of inversion-related molecules which were stacked along the *a*-axis. C-H…O interactions further stabilized the crystal packing.

The structure of 5 – Hydroxy – 7 – methoxy – 2 - (4 - methoxyphenyl) - 4*H* – 1 – benzopyran – 4 – one crystallizes in the $P2_1/c$ space group. The benzopyran - 4 - one ring system and the methoxyphenyl substituent are approximately coplanar. The molecules are linked *via* intermolecular C-H…O hydrogen bonds to form chains along the *a*–axis.

The structure of 5,7 – Dimethoxy – 2 – phenyl - 4*H* – 1 – benzopyran – 4 - one chloroform solvate is stabilized by π-π interactions between the benzopyran - 4 - one ring systems of inversion-related molecules which were stacked along the *c*-axis. C-H…O and C-H…π interactions further stabilized the crystal packing. The crystal has a space group of $P2_1/c$.

The compound of 4’ – Hydroxy – 5 – methoxy - 6,7 – methylenedioxyisoflavone forms an infinite one-dimensional zigzag-like chain developing parallel to *b* axis through O-H…O hydrogen bonds. The chains are stacked along the *c*-axis. The crystal structure is further stabilized by weak π-π and C-H…π interactions. The compound crystallizes out in the space group $P2_1/c$.

The compound of 14 – Deoxy - 11,12 – didehydro - 3,19 – isopropylideneandrographolide crystallizes out in the space group of $P2_12_12_1$. All the six-membered rings in the structure adopt chair comformations. The crystal structure is stabilized by C-H…O interactions, which form a two-dimensional network parallel to *ab* plane.

CHAPTER 1
INTRODUCTION

Single crystal X-ray crystallography method had been employed to determine the crystal structures of five natural products. The crystal data was collected using the *APEX-2 CCD* diffractometer (Bruker, 2005) at the X-ray Crystallography Unit, School of Physics, Universiti Sains Malaysia (USM). Low temperature data were collected using the Oxford Cryosystem Cobra low-temperature attachment.

The samples used were obtained from fellow researchers from HEJ Research Institute of Chemistry, International Centre for Chemical Sciences, University of Karachi, Pakistan; Department of Chemistry, Faculty of Science, Prince of Songkla University, Thailand and Laboratory of Natural Products, Institute of Bioscience and Department of Biomedical Sciences, Faculty of Medicine and Health Science, Universiti Putra Malaysia, Malaysia.

Brief discussion on the basic concepts of X-ray crystallography is included in this chapter. Discussion on some natural products and their benefits are also presented. Natural products are useful in many ways, especially in the development of organic and medicinal chemistry. Finally, the objective of this research is outlined at the end of this chapter.

1.1 X-ray Crystallography

Crystallography is a branch of science that deals with the structures and properties of the crystalline state. Crystals play a vital role in areas such as physics, chemistry, mineralogy, geophysics and materials science. The study of crystals has

been going on for hundreds of years. Crystals usually have characteristic polyhedral shapes and bounded by flat faces. The beauty of crystals is because of the face development.

Earliest contributions to crystallography were based on observations of shapes, and the study of morphology is important to recognize and identify specimens. Nevertheless, faces can be destroyed and it is not essential to a modern definition of a crystal. Besides, crystals are normally too small to be viewed without a high-powered microscope. In addition, majority of crystals are composed of thousands of tiny crystals (polycrystalline).

The following gives a more precise definition to distinguish crystalline from non-crystalline material. In a crystalline material, atoms are arranged in a periodic array over large atomic distances. Long-range order exists. The atoms will position themselves in a repetitive three-dimensional pattern upon solidification, in which each atom is bounded to its nearest-neighbor atoms. On the other hand, long-atomic order is absent in a non-crystalline (amorphous) material. Such materials lack a systematic and regular arrangement of atoms over relatively large atomic distances.

X-ray crystallography is the study of crystal structure by means of X-ray diffraction. X-rays were discovered by German physicist, Wilhelm Conrad Röntgen in 1895 and were so called due to their unknown nature at that time. The first Nobel prize for physics was awarded to Röntgen in 1901 for his momentous discovery. The fact that X-rays are electromagnetic waves of short wavelength came from experiments on the X-ray diffraction by crystals proposed by German scientist, Max

von Laue in 1912. It was later further developed by W.H. Bragg and his son W.L. Bragg.

1.2 Production of X-rays

X-rays are electromagnetic radiation with wavelength, λ in the range of 0.1 to 100Å (1Å = 10^{-10} meters). They are produced when fast-moving electrons collide with a metal target. An X-ray tube consists of a source of electrons, a high accelerating voltage and a metal target. Most of the kinetic energy of the electrons is converted into heat in the target. As such, the latter must be water-cooled in order to prevent it from melting.

There are two electrodes in any X-ray tubes: (a) an anode (the metal target) which is maintained at ground potential and (b) a cathode which is maintained at a high negative potential, usually ranges from 30 to 50 kV for diffraction work.

Basically, X-ray tubes can be divided into two types, depending on the way electrons are provided: (a) filament tubes, in which the source of electrons is a hot filament, and (b) gas tubes, in which electrons are produced by the ionization of a small quantity of gas in the tube. Gas tubes are no longer in use nowadays.

Filament tubes are more widely used. It was invented by W.D. Coolidge in 1913. The internal construction of a filament X-ray tube is shown in Fig. 1.1. It consists of an evacuated glass envelope which insulates the cathode (tungsten filament) at one end from the anode (metal target) at the other. One lead of the high

voltage transformer is connected to the filament and the other to ground. Meanwhile, the target is grounded by its own water-cooling connection.

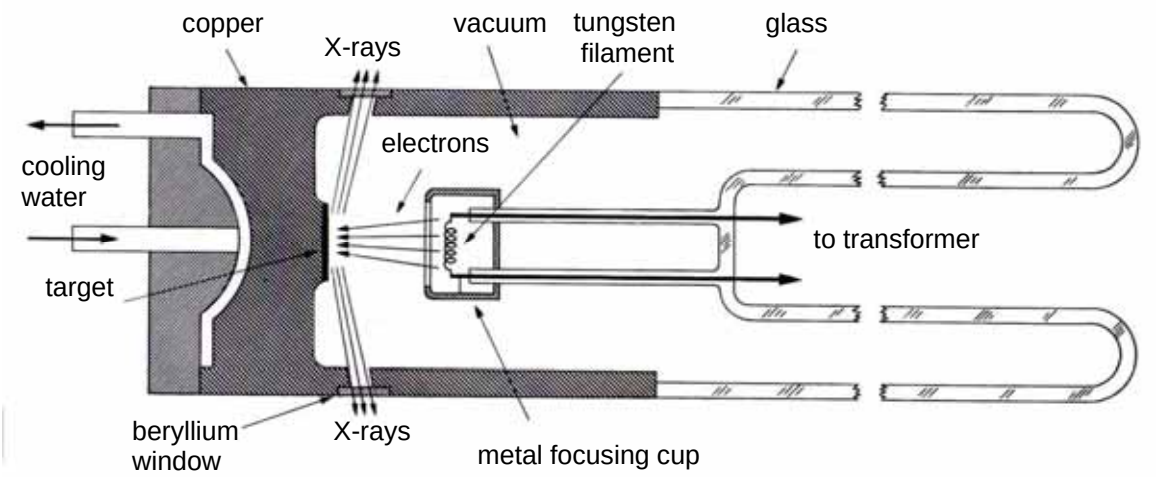

Fig. 1.1 Cross section of filament X-ray tube (Cullity, 1967).

The filament is heated by a filament current of about 3A. Electrons are emitted from the filament and accelerated to the target by high voltage across the tube. The filament is surrounded by a small metal cup which is maintained at the same high negative voltage as the filament. Thus, it repels the electrons and tends to focus them into a narrow region of the target (focal spot). X-rays are emitted from the focal spot and escape from the tube through two or more windows. The windows are transparent to X-rays and vacuum tight. It is normally made of beryllium.

The dissipation of heat at the anode is quite large (500-1500W) and this limits the power which can be applied. Therefore, the rotating anode tubes are sometimes used to increase the output and reduce the time needed to obtain the data. The electron beam is directed onto the edge (or face) of a rotating wheel of the target material. The origin of the X-rays remains in a fixed location but the anode

moves under it. Thus, the heat load can be spread over a much larger area. These tubes can handle at least ten times the power of those with stationary anodes.

1.3 X-ray diffraction

W. L. Bragg noticed the similarity of diffraction to ordinary reflection while engaged in experimental studies in 1912. Hence, he deduced a simple equation treating diffraction as “reflection” from planes in the lattice. For simplicity, Fig. 1.2 shows only two parallel crystal planes, P_1 and P_2. The inter-planar spacing is given as d. Parallel rays, 1 and 2 are incident at an angle θ with these planes. Electrons assumed at O and C is forced to vibrate by the oscillating field of the incident beam. As vibrating charges, it will radiate in all directions.

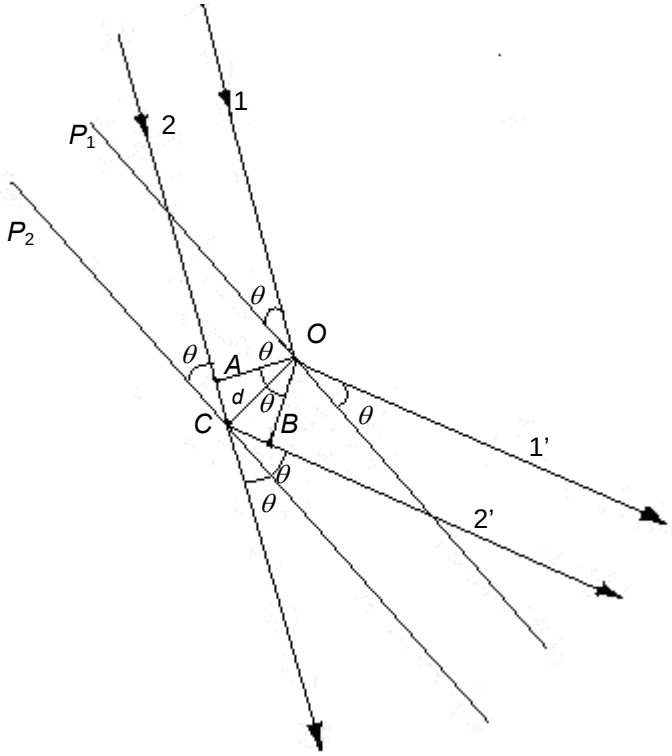

Fig. 1.2 Construction showing conditions for diffraction (Stout & Jensen, 1989)

For a particular direction, the parallel secondary rays 1' and 2' will emerge at angle θ as if it is reflected from the planes. A diffracted beam of maximum intensity is resulted if the waves represented by these rays are in phase. It is clear that $\angle AOC = \angle BOC = \theta$ by dropping perpendiculars from *O* to *A* and *B*, respectively. As such, *AC* = *BC* and waves in ray 2' will be in phase with those in 1' if the difference in path lengths, *AC* + *CB* (=2*AC*) is equal to an integral number of wavelengths λ.

This equality is expressed by

$$2AC = n\lambda \qquad n = 1, 2, 3,\ldots \tag{1.1}$$

where *n* is an integer.

It is known that $AC/d = \sin\theta$. By substitution in equation (1.1),

$$2d\sin\theta = n\lambda \qquad n = 1, 2, 3,\ldots \tag{1.2}$$

This is Bragg's law.

Since $\sin\theta$ must be equal to or less than 1,

$$\frac{n\lambda}{2d} = \sin\theta \leq 1 \tag{1.3}$$

Thus for *n* = 1,

$$\lambda \leq 2d \tag{1.4}$$

Therefore, the X-rays used for diffraction must have wavelengths comparable to or smaller than the inter-atomic spacing in the crystal. Otherwise, diffraction will not be observed.

Ewald sphere (Fig. 1.3) was introduced by P.P. Ewald. For a crystal C and an X-ray beam of wavelength λ, let $\mathbf{s}_o$ be the unit vector in the direction of the primary beam and **s** be the unit vector of the diffracted beam concerning a lattice plane with the normal vector **h**. Hence, the vectors **h**, $\mathbf{s}_o$ and **s** give the equation

$$\mathbf{h} = \frac{\mathbf{s} - \mathbf{s}_o}{\lambda} \qquad (1.5)$$

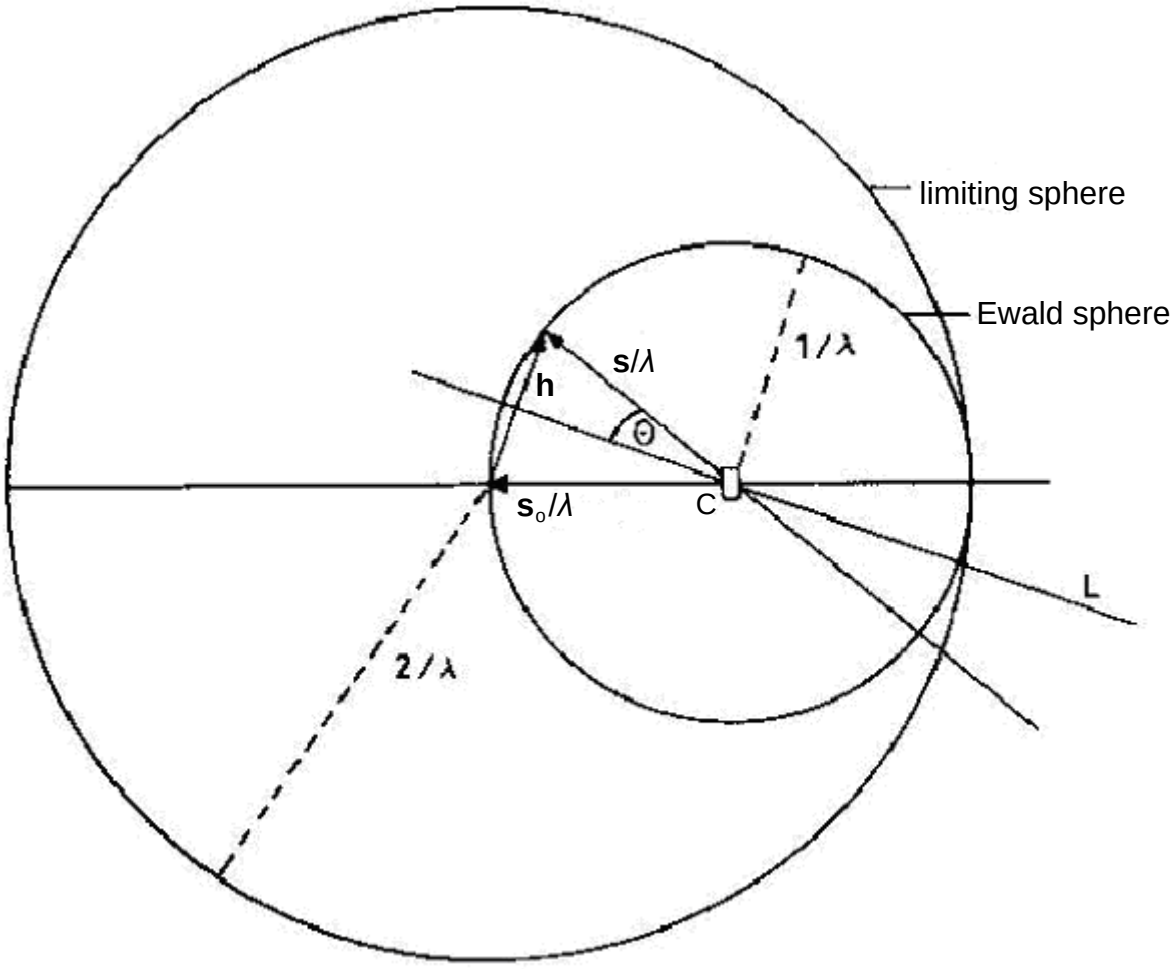

Fig 1.3 Ewald sphere, radius 1/λ and limiting sphere,radius 2/λ (Luger, 1980)

It is found that

$$\frac{|\mathbf{h}|/2}{1/\lambda} = \sin\theta \qquad (1.6)$$

and with

$$d = \frac{1}{|\mathbf{h}|} \qquad (1.7)$$

we get $\lambda = 2d \sin \theta$ (Bragg's law). For diffraction to take place, Ewald states that a lattice plane L must be in the diffraction position such that its normal vector **h** is on the surface of a sphere of radius 1/λ around C, which is the Ewald sphere. Diffraction of a lattice plane L happens only if d (reciprocal of the normal vector's magnitude), satisfies Bragg's law. In other words, the reciprocal lattice points must touch the surface of the Ewald sphere in order for diffraction to occur.

The plane L acts like a reflection from a mirror, in the sense that the angle to the plane of the incident and the reflected beams are similar. X-rays are reflected by the lattice planes of a single crystal only if the angle of the incident beam to the plane fulfills the conditions for Bragg's reflection. Since $|\sin\theta| \leq 1$, thus from (1.6),

$$|\mathbf{h}| \leq 2/\lambda \qquad (1.8)$$

It follows that the number of possible reflections for a given radiation with fixed wavelength λ is limited. Since the diameter of Ewald sphere is 2/λ, only those reflections in reciprocal lattice space inside the sphere of radius 2/λ (the limiting sphere) can be observed. The radius of the limiting sphere is twice of that of the Ewald sphere (Fig. 1.3). If there is only one reflection per one reciprocal unit cell, the total reflections inside the limiting sphere, *M*, is

$$M = \frac{4}{3}\pi\left(\frac{2}{\lambda}\right)^3 \frac{1}{V^*} \tag{1.9}$$

$$M = \frac{32\pi}{3}\frac{1}{\lambda^3}\frac{1}{V^*} \tag{1.10}$$

$$M = \frac{35.5}{\lambda^3}V \tag{1.11}$$

where $V = 1/V^*$ = cell volume.

1.4 Natural Product

Natural products are natural occurring chemical compounds which can be found in plants, flowers, animals, insects and other microorganisms. The study of natural products has been going on since prehistoric times. The search of new natural sources still persists even today as it plays a key role in the development of drugs.

Shen Nung (2800 BC) compiled the first medicinal herbal, the *Pen-Tsao*, and describes 365 drugs used in those days. Meanwhile, the Papyrus of Elbers (1500 BC) describes several preparations of natural products. It was one of the most complete medical documents existing during the Egyptians empire. In the north of Mediterranean, Pedanius Dioscorides studied the medical uses of hundreds of plants. He wrote *materia medica* during the first century.

In the 19th century, the isolation and identification of natural products became more systematic. The art of synthesis was transformed from the apothecaries to the expert chemists. Simultaneously, the quality of the products improved. Most of the natural products are isolated from plant origins. The common procedure involved and still in use is described as follows.

The plant material is divided according to the plant parts. Then, the material is dried and ground to a suitable particle size. The dry material is extracted by the use of suitable solvent such as chloroform or methanol. The organic extract is then concentrated. The crude extract may contain hundreds of compounds. Earlier, the separation process was based on crystallization or distillation techniques. Later, the separation process has been facilitated by the development of modern chromatographic methods. In practice, almost all the components can be isolated in pure form.

Structural complexity has been the driving force for the development of spectroscopic means of structure elucidation (Ari Koskinen, 1993). The proponents of X-ray crystallography and other spectroscopies have claimed to be the most powerful techniques in providing a rapid and reliable means of establishing the structure of a new compound. In most cases, the absolute stereochemistry of the compound can be ascertained.

In this thesis, the structures of five new natural products were elucidated and the results published in ISI-citation-indexed journals. These natural products are:-

1.4.1 3,5,7-Trimethoxy-2-phenyl-4*H*-1-benzopyran-4-one; (I)

The title compound, (I), a flavone, is a secondary metabolite occuring in plants. Some flavones show antimycobacterial activity (Yenjai *et al*., 2004). Compound (I) was isolated from the rhizomes of *Kaempferia parviflora*, which were collected from Loei province in the north-eastern part of Thailand. It was previously isolated from the black rhizomes of *Boesenbergia pandurata* (Jaipetch *et al*., 1983). Compound (I) does not exhibit antiplasmodium, antifungal, antimycobacterial and cytotoxic activities (Yenjai *et al*., 2004).

1.4.2 5-Hydroxy-7-methoxy-2-(4-methoxyphenyl)-4*H*-1-benzopyran-4-one; (II)

The compounds present in *Kaempferia parviflora*, a plant growing in the northeastern part of Thailand have been investigated. Previously, the isolation and crystal structures of two flavanoids from the rhizomes of this plant have been reported (Fun *et al*., 2005; Teh *et al*., 2005*a*). The title compound, (II) was also isolated from the rhizomes of *Kaempferia parviflora*, which were collected from Loei province in the north-eastern part of Thailand.

Compound (II), a known flavone, is a secondary metabolite occurring in plants. It does not exhibit antiplasmodium, antifungal, antimycobacterial and cytotoxic activities against KB (oral human epidermoid carcinoma), BC (breast cancer) and NCI-H187 (human small cell lung cancer) cell lines (Yenjai *et al*., 2004).

1.4.3 5,7-Dimethoxy-2-phenyl-4*H*-1-benzopyran-4-one chloroform solvate; (III)

Crystal structures of three flavonoids (Fun *et al*., 2005; Teh *et al*., 2005*a*,*b*), from *Kaempferia parviflora* or 'Kra Chai Dam' in Thai, which is a medicinal plant growing in the north-eastern part of Thailand have been reported previously. Flavonoids are the main components of this plant. The title compound, (III) is another flavonoid which was isolated from the rhizomes of the same plant. This compound was previously isolated from aerial parts of *Helichrysum nitens* (Francisco *et al*., 1988).

1.4.4 4'-Hydroxy-5-methoxy-6,7-methylenedioxyisoflavone; (IV)

Iris germanica Linn. belongs to the family Iridaceae. *Iris* is a rhizomatous or bulbous herb. The genera include commercially valuable ornamentals. Historically, the plant was used to treat constipation, dermatitis and skin disease. *Iris* species are also reported to have various biological activities, including cytotoxic, anticancer, anti-ulcer, piscicidal and insecticidal activities (Miyake *et al*., 1997; Takahashi *et al*., 1999; Wong *et al*., 1985, 1986; Muto *et al*., 1994; Takahashi *et al*., 1993).

The plant contains isoflavones such as irisolidone, irisolidone 7-*O*-α-D-glucoside, irilone, iriflogenin, iriskashmirianin, irigenin and the title compound, nigricin, (IV) (Wollenweber *et al*., 2003; Orhan *et al*., 2003; Atta-ur-Rahman *et al*., 2003). The plant possesses anti-inflammatory and hypolipidemic activity (Atta-ur-Rahman *et al*., 2003; Choudhary *et al*., 2005). Nigricin has also been reported for its bactericidal activity against *Staphylococcus aureus* and *Pseudomonas aeruginosa* (Atta-ur-Rahman *et al*., 2003).

1.4.5 14-Deoxy-11, 12-didehydro-3, 19-isopropyledineandrographolide; (V)

Andrographis paniculata Nees (Acanthaceae) is a very popular herb commonly used in Indian Ayurvedic and Chinese traditional medicine for the treatment of a variety of illnesses. Extracts of this plant have been shown to possess anti-inflammatory (Shen *et al*., 2002), antiviral (Chang *et al*., 1991; Calabrese *et al*., 2000), immunostimulatory (Puri *et al*., 1993; See *et al*., 2002), hypoglycaemic (Zhang & Tan, 2000), hypotensive (Zhang & Tan, 1996) and anticancer (Siripong *et al*., 1992; Stanslas *et al*., 2001; Kumar *et al*., 2004) activities. The main labdane type diterpenoid constituents of this plant are andrographolide, neoandrographolide, 14 - deoxyandrographolide and 14 – deoxy - 11, 12 - didehydroandrographolide.

During the course of developing andrographolide analogues with significant pharmacological activities, the title compound, (V) was semisynthesised by reacting compound 14-Deoxy-11, 12-didehydroandrographolide with 2, 2-dimethoxypropane under reflux.

1.5 Research Objective

The objective of this research is to get the 3D structure of five newly discovered natural products. Basically, this study involves the determination of crystal structures through X-ray crystallography. This technique provides detailed information of the crystal structures. Structure conformation and geometrical parameters such as bond distances, bond angles and torsion angles can be obtained easily. In addition, the crystal packing of these molecules and their packing forces can be elucidated:

a) As part of the ongoing studies on the structure and biological activities of Thai medicinal plants (Chantrapromma *et al*., 2003, 2004, 2005; Boonnak *et al*., 2005; Fun *et al*., 2005; Teh *et al*., 2005*a*,*b*; Cheenpracha *et al*., 2005; Ng *et al*., 2005*a*,*b*; Pakhathirathien *et al*., 2005), we have undertaken the X-ray crystal structure determination of (I), (II) and (III). The structure-activity relationship (SAR) of these flavonoids will be further studied by the Thai researchers.

b) The X-ray structure analysis of (IV) was undertaken to establish its molecular structure and stereochemistry.

c) The X-ray crystal structure analysis of (V) was undertaken in order to establish its molecular structure and stereochemistry.

d) The results obtained from this research are able to assist other researchers in developing appropriate and better drugs in the near future.

CHAPTER 2
BASICS OF X-RAY STRUCTURE ANALYSIS

2.0 Introduction

This chapter is concerned with the basics of x-ray structure analysis which includes the atomic scattering factor, structure factor, heavy atom method, direct method, data reduction and refinement.

2.1 Argand Diagram

An Argand diagram can be used to represent the combination of waves clearly and concisely. The waves are represented as vectors with real and imaginary components.

Hence,

$$\mathbf{f_1} = f_1\cos\varphi_1 + \mathrm{i}f_1\sin\varphi_1 \qquad (2.1)$$

$$\mathbf{f_2} = f_2\cos\varphi_2 + \mathrm{i}f_2\sin\varphi_2 \qquad (2.2)$$

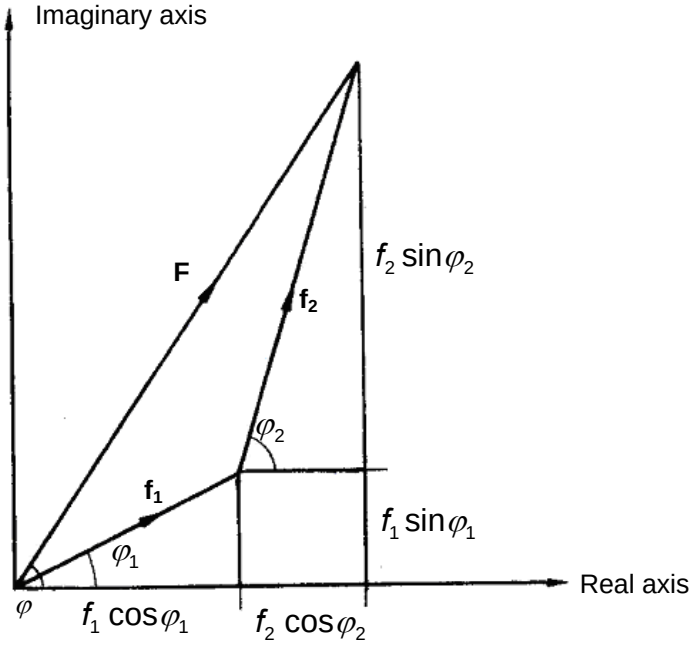

Fig. 2.1 Combination of two waves as vectors on an Argand diagram. **F** is the resultant vector (Ladd & Palmer, 1979)

De Moive's theorem is given by

$$e^{\pm i\varphi} = \cos\varphi \pm i\sin\varphi \tag{2.3}$$

This theorem provides a more convenient summation for $\mathbf{f_1}$ and $\mathbf{f_2}$

$$\mathbf{f_1} = f_1 e^{i\varphi_1} \ , \quad \mathbf{f_2} = f_2 e^{i\varphi_2} \tag{2.4}$$

Thus,

$$\mathbf{F} = f_1 e^{i\varphi_1} + f_2 e^{i\varphi_2} = F e^{i\varphi} \tag{2.5}$$

where

$$F\sin\varphi = f_1 \sin\varphi_1 + f_2 \sin\varphi_2 \tag{2.6}$$

$$F\cos\varphi = f_1 \cos\varphi_1 + f_2 \cos\varphi_2 \tag{2.7}$$

2.2 Combination of *N* Waves

Combination of any number of waves is possible by extending the foregoing analysis. From (2.5), the resultant of *N* waves is

$$\mathbf{F} = f_1 e^{i\varphi_1} + f_2 e^{i\varphi_2} + f_3 e^{i\varphi_3} + ... + f_j e^{i\varphi_j} + ... + f_N e^{i\varphi_N} \tag{2.8}$$

or

$$\mathbf{F} = \sum_{j=1}^{N} f_j e^{i\varphi_j} \tag{2.9}$$

Equation (2.9) expresses a polygon of vectors (Fig. 2.2), on an Argand diagram and the resultant **F** is given by

$$\mathbf{F} = |F| e^{i\varphi} \tag{2.10}$$

where

$$F\sin\varphi = \sum_{j=1}^{N} f_j \sin\varphi_j \tag{2.11}$$

$$F\cos\varphi = \sum_{j=1}^{N} f_j \cos\varphi_j \tag{2.12}$$

The amplitude $|F|$ is

$$|F|^2 = \mathbf{FF^*} \tag{2.13}$$

in which $\mathbf{F^*}$ is the complex conjugate of **F**:

$$\mathbf{F^*} = |F|\, e^{-i\varphi} \tag{2.14}$$

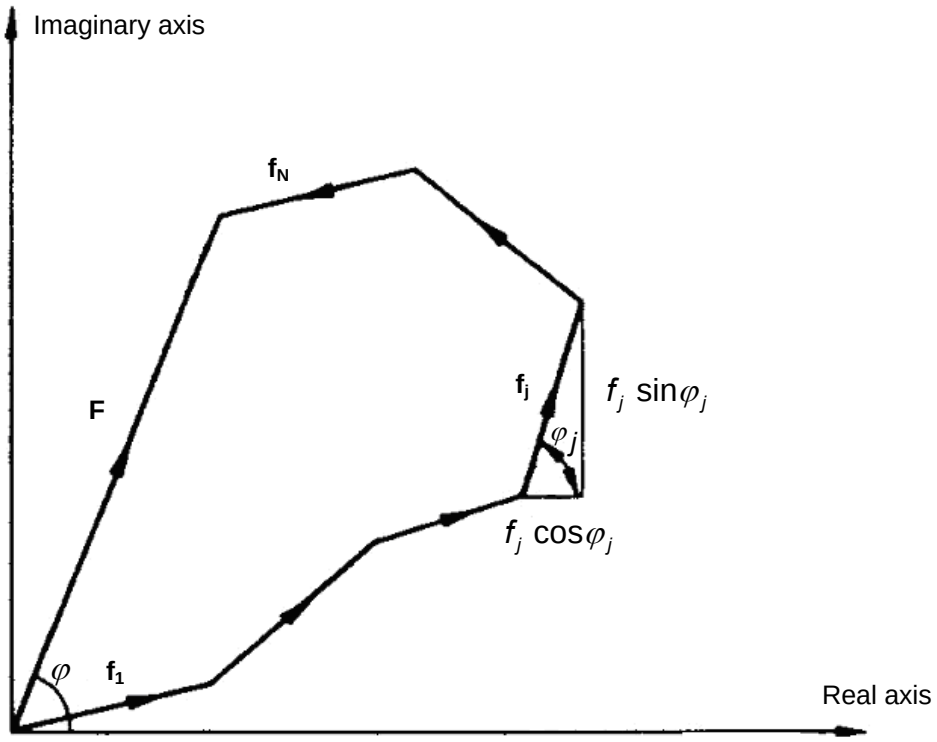

Fig. 2.2 Combination of N waves (N = 6) on an Argand diagram (Ladd & Palmer, 1979)

2.3 Phase Difference

The path difference associated with waves scattered by an atom j whose position relative to the origin is specified by the coordinates x_j, y_j, z_j is given as

$$\delta_j = \lambda(hx_j + ky_j + lz_j) \tag{2.15}$$

The corresponding phase difference is

$$\varphi_j = (2\pi/\lambda)\ \delta_j \tag{2.16}$$

or

$$\varphi_j = 2\pi\,(hx_j + ky_j + lz_j) \tag{2.17}$$

2.4 Scattering by Atoms

The amplitudes of the waves scattered by the atoms (the atomic scattering factor) is needed in order to evaluate the combined scattering from the atoms in the unit cell. It is tabulated as functions of $(\sin\theta)/\lambda$ and denoted as $f_{j,\theta}$ or f_j. The atomic scattering factor depends on the nature of the atom, the scattering direction, the wavelength of X-rays used and the thermal vibrations of the atom.

The atomic scattering factor, *f*, depends on the number of electrons in the atom. The maximum value for a given atom *j* is Z_j, the atomic number of the *j* th atomic species. Along the direction of the incident beam $\left[\sin\theta(hkl)=0\right]$, *f* has maximum value:

$$f_{j,\theta(\theta=0)} = Z_j \tag{2.18}$$

f is measured in electrons.

In general, each atom in a given crystal vibrates due to thermal energy. By assuming isotropic vibration, the temperature factor correction to the atomic scattering factor for the *j* th atom is

$$T_{j,\theta} = \exp[-B_j(\sin^2\theta)/\lambda^2] \tag{2.19}$$

B_j, the temperature factor of atom *j* is given by

$$B_j = 8\pi^2\overline{U_j^2} \tag{2.20}$$

where $\overline{U_j^2}$ is the mean square amplitude of vibration of the *j* th atom from its equilibrium position in a direction normal to the reflecting plane. It is a function of temperature. Like *f*, the factor *T* is a function of $(\sin\theta)/\lambda$. The temperature-corrected atomic scattering factor may be written as

$$g_j = f_{j,\theta} T_{j,\theta} \tag{2.21}$$

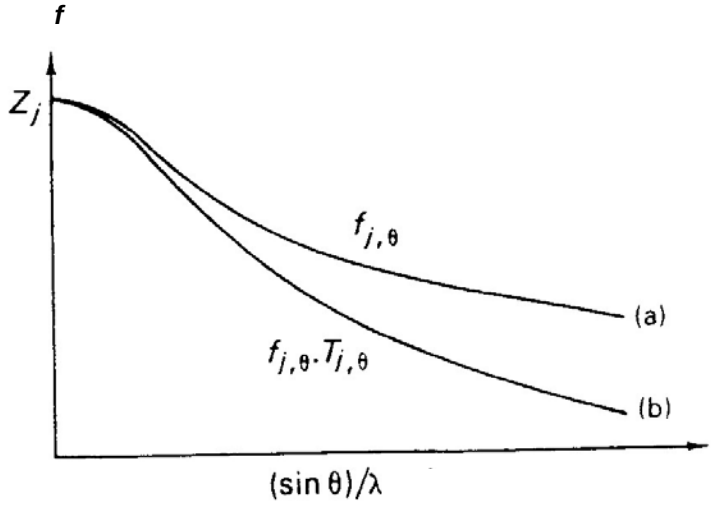

Fig. 2.3 Atomic scattering factors: (a) stationary atom, $f_{j,\theta}$ (b) atom corrected for thermal vibration, $f_{j,\theta} T_{j,\theta}$. (Ladd & Palmer, 1979).

2.5 Structure Factor

The structure factor **F**(*hkl*) expresses the combined scattering of all atoms in the unit cell compared to that of a single electron. Its amplitude $|F(hkl)|$ is measured in electrons (Ladd & Palmer, 1979). The components needed for the combined scattered wave from the *(hkl)* planes are $g_{j,\theta}$ and $\phi_j(hkl)$. Often, it is referred to as g_j dan ϕ_j, respectively. The individual scattered waves from the various atoms *j* are vectors of the form given in (2.8). The resultant wave for the unit cell is

$$\mathbf{F}(hkl) = \sum_{j=1}^{N} g_j e^{i\varphi_j} = \sum_{j=1}^{N} g_j e^{\left[i2\pi(hx_j + ky_j + lz_j)\right]} \tag{2.22}$$

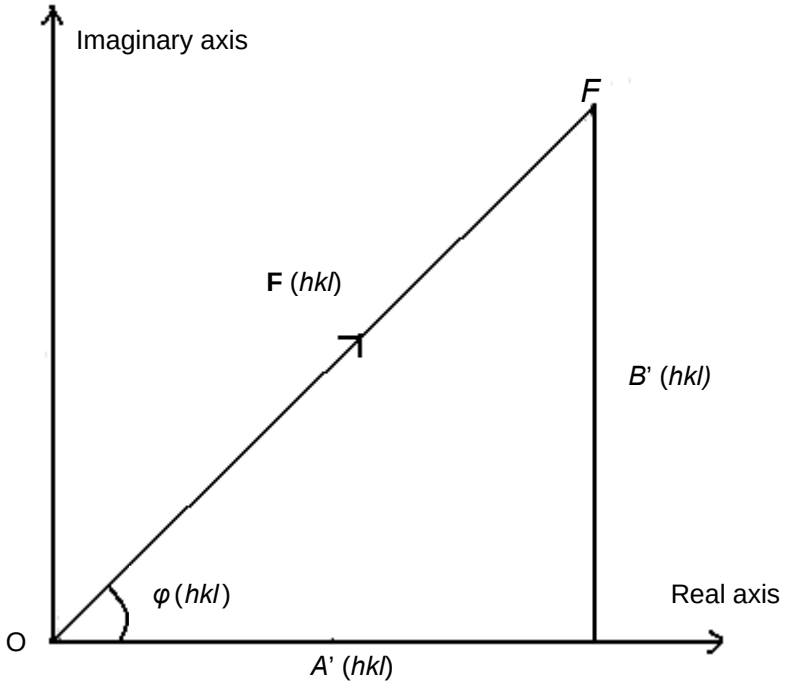

Fig. 2.4 Structure factor **F***(hkl)* plotted on an Argand diagram; φ *(hkl)* is the resultant phase, and the amplitude |***F****(hkl)*| is represented by OF (Ladd & Palmer,1979).

From Fig. 2.4,

$$\mathbf{F}(hkl) = A'(hkl) + iB'(hkl) \tag{2.23}$$

in which $$A'(hkl) = \sum_{j=1}^{N} g_j \cos 2\pi(hx_j + ky_j + lz_j) \tag{2.24}$$

and $$B'(hkl) = \sum_{j=1}^{N} g_j \sin 2\pi(hx_j + ky_j + lz_j) \tag{2.25}$$

By comparison with (2.10), we may write

$$\mathbf{F}(hkl) = |F(hkl)|\, e^{i\varphi(hkl)} \tag{2.26}$$

where the amplitude is given by

$$|F(hkl)| = \left[A'^2(hkl) + B'^2(hkl)\right]^{\frac{1}{2}} \tag{2.27}$$

and the phase by

$$\tan\varphi(hkl) = B'(hkl)/A'(hkl) \tag{2.28}$$

It can be seen from Fig. 2.4 that

$$A'(hkl) = |F(hkl)|\cos\varphi(hkl) \tag{2.29}$$

$$B'(hkl) = |F(hkl)|\sin\varphi(hkl) \tag{2.30}$$

2.6 Limiting Conditions and Systematic Absences

For a body-centered unit cell, an atom at x_j, y_j, z_j is related by translation to another atom (of the same type) at $\frac{1}{2}+x_j$, $\frac{1}{2}+y_j$, $\frac{1}{2}+z_j$. If there are N atoms in the unit cell, summation for the $N/2$ atoms not related by translation is given by

$$\mathbf{F}(hkl) = \sum_{j=1}^{N/2} g_j \left\{ \exp[\,i2\pi\,(hx_j + ky_j + lz_j)] + \exp[i2\pi\,(hx_j + ky_j + lz_j + \frac{1}{2}(h+k+l))] \right\} \tag{2.31}$$

The term in { } can be written as

$$\left\{\exp[\,i2\pi\,(hx_j + ky_j + lz_j)]\right\}\left\{1+\exp[i\pi\,(h+k+l)]\right\} \tag{2.32}$$

$(h + k + l)$ = integer = m. Thus,

$$1+e^{i\pi(h+k+l)} = 1+\cos(m\pi) \tag{2.33}$$

It is known that

$$1+\cos(m\pi) = 2\cos^2(m\pi/2) \tag{2.34}$$

and

$$2\cos^2(m\pi/2) = 2\cos^2\left[2\pi\,(h+k+l)/4\right] = G(hkl) \tag{2.35}$$

As such, the reduced structure factor equation for a body-centered unit cell can be expressed as

$$F(hkl) = 2\,cos^2\,[\,2\pi\,(h+k+l)/4\,]\sum_{j=1}^{N/2} g_j\,\exp\,[\mathrm{i}2\pi\,(hx_j + ky_j + lz_j)\,] \qquad (2.36)$$

$G(hkl) = 2\cos^2\,[2\pi(h+k+l)/4]$ can only take two values, i.e.,

$$G(hkl) = 2 \qquad (2.37)$$

if $h + k + l$ is an even number and

$$G(hkl) = 0 \qquad (2.38)$$

if it is odd.

Hence, the limiting conditions for a body-centered unit cell (the conditions under which reflection can occur) can be written as

$$hkl\text{: } h + k + l = 2n \quad (n = 0, \pm 1, \pm 2, \ldots) \qquad (2.39)$$

The same situation expressed in terms of systematic absences (the conditions under which reflection cannot occur) is

$$hkl\text{: } h + k + l = 2n + 1 \qquad (2.40)$$

For any unit-cell type, expressions analogous to (2.36) can be derived. Table 2.1 gives the limiting conditions for some of the unit-cell type. The limiting conditions for 2_1 screw axis are shown in Table 2.2. For glide planes, the limiting conditions are given in Table 2.3.

Table 2.1 Limiting Conditions for Some of the Unit-Cell Type

Unit-cell type	Limiting conditions	Translations associated with the unit-cell type	$G(hkl)$
P	None	None	1
A	$hkl : k + l = 2n$	$b/2 + c/2$	2
B	$hkl : h + l = 2n$	$a/2 + c/2$	2
C	$hkl : h + k = 2n$	$a/2 + b/2$	2
I	$hkl : h + k + l = 2n$	$a/2 + b/2 + c/2$	2
F	$hkl : h + k = 2n$ $hkl : k + l = 2n$ $hkl : (h + l = 2n)$* (These conditions imply h, k, l all even or all odd).	$a/2 + b/2$ $b/2 + c/2$ $a/2 + c/2$	4

* This condition is not independent of the other two.

Table 2.2 Limiting Conditions for 2_1 Screw Axes

Screw axis	Orientation	Limiting condition	Translation component
2_1	$//a$	$h00 : h = 2n$	$a/2$
2_1	$//b$	$0k0 : k = 2n$	$b/2$
2_1	$//c$	$00l : l = 2n$	$c/2$

Table 2.3 Limiting Conditions for Glide Planes

Glide plane	Orientation	Limiting condition	Translation component
a	$\perp b$	$h0l : h = 2n$	*a*/2
a	$\perp c$	$hk0 : h = 2n$	*a*/2
b	$\perp a$	$0kl : k = 2n$	*b*/2
b	$\perp c$	$hk0 : k = 2n$	*b*/2
c	$\perp a$	$0kl : l = 2n$	*c*/2
c	$\perp b$	$h0l : l = 2n$	*c*/2
n	$\perp a$	$0kl : k + l = 2n$	*b*/2 + *c*/2
n	$\perp b$	$h0l : h + l = 2n$	*a*/2 + *c*/2
n	$\perp c$	$hk0 : h + k = 2n$	*a*/2 + *b*/2

2.7 Friedel's Law

The centrosymmetric property of the diffraction pattern is stated by Friedel's law as $I(hkl) = I(\bar{h}\bar{k}\bar{l})$. For both, hkl and $\bar{h}\bar{k}\bar{l}$ reflections, g_j will be the same because the atomic scattering factor is a function of $[(\sin\theta)/\lambda]^2$, i.e.

$$g_{j,\theta} = g_{j,-\theta} \tag{2.41}$$

because reflection from opposite sides of any plane will occur at the same Bragg angle θ. From (2.22),

$$\mathbf{F}(hkl) = \sum_{j=1}^{N} g_{j,\theta} \exp[\mathrm{i}2\pi(hx_j + ky_j + lz_j)] \tag{2.42}$$

and

$$\mathbf{F}(\bar{h}\bar{k}\bar{l}) = \sum_{j=1}^{N} g_{j,-\theta} \exp[-\mathrm{i}2\pi(hx_j + ky_j + lz_j)] \tag{2.43}$$

From (2.23),

$$\mathbf{F}(\bar{h}\bar{k}\bar{l}) = A'(\bar{h}\bar{k}\bar{l}) + \mathrm{i}B'(\bar{h}\bar{k}\bar{l}) \tag{2.44}$$